MECHANISMS OF POLARIZATION SWITCHING IN SINGLE-TRANSVERSE-MODE VCSELS: THERMAL SHIFT AND NONLINEAR SEMICONDUCTOR DYNAMICS

S. Balle, E. Tolkachova, M. San Miguel, J. R. Tredicce, J. Martín-Regalado and A. Gahl

Instituto Mediterráneo de Estudios Avanzados, IMEDEA (CSIC-UIB),
Universitat de les Illes Balears, E-07071 Palma de Mallorca, Spain

Abstract

We analyze polarization switching in Vertical Cavity Surface Emitting Lasers taking into account a proper semiconductor frequency-dependent complex susceptibility and spin-flip processes. Thermal effects are included as a varying detuning, and gain differences arise from birefringence splitting. We find that for large birefringence, gain differences between the two linearly polarized modes are preponderant and switching occurs due to thermal shift. For small birefringence, a polarization switching from the high-gain to the low-gain mode occurs due to the combined effect of birefringence and semiconductor phase-amplitude coupled dynamics for a finite value of the carrier spin flip rate.

Vertical Cavity Surface Emitting Lasers[1] typically emit linearly polarized (LP) light and, for bias currents relatively close to threshold, in the fundamental transverse mode. With this transverse profile fixed, a rich phenomenology of polarization instabilities have been reported.[2–7] Often, the LP mode selected at threshold becomes unstable as the injection current is increased, and a switch to the orthogonal LP mode occurs for some value of the injection current.

A first explanation proposed for the origins of this polarization switching (PS) relies on the different modal gain corresponding to each LP mode.[6] Gain differences appear because of the different frequency of the LP modes in a birefringent optical cavity, but they can also be due to the combined effect of birefringence and spatial-hole burning.[8] At threshold, the LP mode with larger gain is selected. As the injection current is increased, device self-heating induces a red-shift of both the gain curve and the cavity resonances. The red-shift of the gain spectrum is larger than that of the cavity resonances, which may lead to a change of sign in the gain difference between the two LP modes, and thus to PS.[6] This is a rather intuitive argument, but there are some experiments which cannot be explained within this framework. In particular, PS still occurs in a geometry which tends to equalize the gain of the two LP modes and when the cavity resonance is always detuned to the same side of the gain peak.[7] Moreover, PS has also been observed when driving the laser with electrical pulses shorter than the thermal relaxation time, so that thermal shifts do not come into play.[9]

A second mechanism proposed for explaining PS invokes the combined effect of birefringence and saturable dispersion associated with the linewidth enhancement factor, α, in the context of a Spin Flip Model (SFM) for the nonlinear gain dynamics of the semiconductor medium.[10,11] Small gain differences select a LP at threshold but, as the injection current is increased, they are easily overcome by phase-amplitude dynamics.[10,11] However, this model does not incorporate a frequency dependent gain, and therefore it does not take into account either nonlinear gain differences between the LP modes, or the effects of thermal shift of the cavity resonances and the gain peak.

In this paper we develop an extension of the SFM which incorporates a realistic spectral dependence of the gain and index of refraction of active QW structures. We describe the optical field in terms of the slowly varying amplitudes of its circularly polarized components, $E_\pm$, each interacting only with a part, $N_\pm$, of the total carrier density $N = N_+ + N_-$. The carrier densities $N_\pm$ tend to be equalized by spin flip processes. The equalization rate of the holes is much larger than that of the electrons,[12] so we take equal densities for the populations of holes, while the densities of electrons are equalized at a rate γ_j. The interaction of a monochromatic circularly polarized wave and the active QW material is described through a complex susceptibility $\chi_\pm$, which involves a summation over all $k-$states in the first Brillouin zone weighted with the carrier occupancy of each state.[13] Such a susceptibility can be analytically evaluated when some simplifying assumptions are made:[14] 1) the dipole matrix element between the valence and conduction bands is independent of k, 2) the width of each transition is also independent of k, 3) all carriers are in quasi-equilibrium within each band, and 4) low temperature limit. Then, when only one electron and one hole (parabolic) bands are considered it is found that

$$\chi_\pm = -\chi_0 \left[\ln\left(1 - \frac{2D_\pm}{u_\pm + i}\right) + \ln\left(1 - \frac{D_+ + D_-}{u_\pm + i}\right) - \left(1 - \frac{b}{u_\pm + i}\right)\right], \quad (1)$$

where $D_\pm \equiv N_\pm/N_t$ is the carrier density per spin orientation normalized to the (total) transparency carrier

density, N_t. The dependence on the frequency of the fields arises through

$$u_{\pm} = \frac{\omega_{\pm}}{\gamma} + \Delta + \sigma \left(\frac{N_+ + N_-}{N_t} \right)^{1/3} , \qquad (2)$$

where $\omega_c + \omega_{\pm}$ are the optical frequencies of each circularly polarized wave, and $\Delta = (\omega_c - \omega_t)/\gamma$ is the detuning between the cavity resonance and the nominal transition frequency normalized to the linewidth, γ, of the optical transitions for fixed k. This linewidth corresponds to the inverse of the dephasing time of the material polarization. Band-gap renormalization effects have been included in (1) through σ which describes the band-gap shrinkage with carrier density. b is linked to the total energy span of the conduction and valence bands and it determines the optical response of the QW material in the absence of carriers, i. e., it sets the background index of refraction and absorption of the unpumped active region. Finally, χ_0 is the device-dependent parameter that determines the material gain. The characteristics of $\chi_{\pm}$ and the approximations made in its derivation have been discussed in detail in [14]. The main advantage of using a susceptibility like (1) is that it allows us to incorporate in a realistic way the nonlinear dependence on carrier density of both the gain and index spectra of the QW material. Hence, it incorporates the effects of the QW active material on both the amplitude and phase of the optical field.

It is worth noting that a primary thermal effect, namely, the relative shift of the cavity frequency and the material gain spectrum, is easily taken into account in (1) by letting Δ to depend on temperature. Since the gain spectrum redshifts faster than the cavity resonance, increasing temperature corresponds to increasing Δ. We consider only temperature changes small enough to neglect thermal changes in material gain and transparency carrier density.

The dynamical evolution equations of the SFM including the spectral dependence of the material response to the optical field are:

$$\dot{E}_{\pm} = -\kappa E_{\pm} + i\frac{\Gamma}{2} a \chi_{\pm} E_{\pm} - i\gamma_p E_{\mp} , \qquad (3)$$

$$\dot{N}_{\pm} = \frac{I}{2} - \gamma_e N_{\pm} - \gamma_j \left(N_{\pm} - N_{\mp} \right) + a\chi_{\pm}^{im} |E_{\pm}|^2 , \quad (4)$$

where we have normalized the fields such that $|E_{\pm}|^2$ corresponds to photon density, κ stands for the total cavity loss, $a = (c/n_g)(\omega_c/cn)$, Γ is the confinement factor to the active region, I is the (total) injected current density, $\chi_{\pm}^{im}$ is the imaginary part of the susceptibility, and γ_e is the carrier decay rate. A proper description of frequency dependent dynamics is obtained solving (3)-(4) while imposing self-consistently that $\omega_{\pm} = i\dot{E}_{\pm}/E_{\pm}$.

Eqs. (3)-(4) together with (1) have steady state solutions which correspond to two orthogonal states of LP emission depending on whether E_+ and E_- lock at a phase difference $\phi = 0$ or π. For definiteness, we label them as $\hat{x}$ or $\hat{y}$, respectively, and for $\gamma_p > 0$ they correspond to the shorter and longer wavelength, respectively, their frequency splitting being roughly $\Delta\omega = 2\gamma_p$. The linear stability analysis of such solutions allows us to determine the domain in parameter space where each LP mode is stable and thus the possible occurrence of PS.

Typical stability results for a relatively large value of the birefringence are shown in Fig. 1 in the $I - \Delta$ plane. There is a minimum threshold for $\Delta = \Delta_m$ corresponding to the cavity resonance being aligned with the gain peak. For a given Δ, the LP mode selected at threshold is the closest to the gain peak, i. e., $\hat{x}$ for $\Delta < \Delta_m$ and $\hat{y}$ for $\Delta > \Delta_m$. Above threshold we find a region (**I**) in which only $\hat{x}$ is stable and another (**III**) where only $\hat{y}$ is stable. A bistability region (**II**) also appears, extending from below to above Δ_m almost symmetrically, due to nonlinear gain saturation induced by the lasing mode. PS occurs as the system is brought from **I** to **III** or viceversa. In this case, PS does not occur at constant Δ. Instead, it occurs for constant I as Δ is varied across Δ_m. Within our framework, we call this PS "thermally induced" since it appears by scanning Δ, either by changing substrate temperature or by device self-heating as the current is increased (see arrow in Fig. 1).

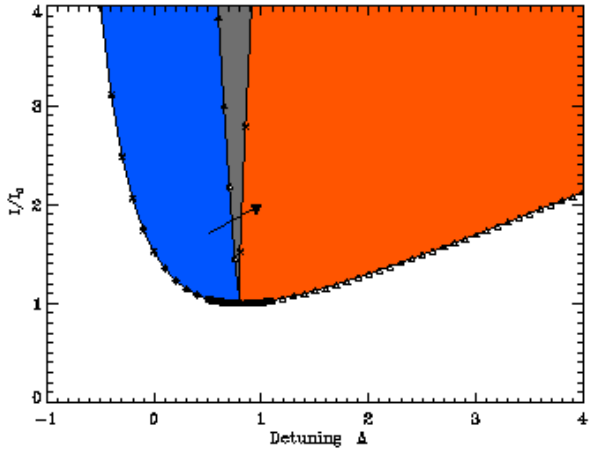

Fig. 1. Stability diagram of LP solutions in the plane $I - \Delta$ (the injection current is normalized to the minimum threshold). Solid arrow indicates a possible path associated with thermal effects. Parameter values: $\gamma_e = 1\ ns^{-1}$, $\gamma_p = 30\ ns^{-1}$, $\gamma_j = 150\ ns^{-1}$, $\kappa = 300\ ns^{-1}$, $\gamma = 10^4\ ns^{-1}$, $\Gamma = 4.5\%$ and $a\chi_0 = 1.3\ 10^4\ ns^{-1}$.

Fig. 2 displays a typical stability diagram correspond-

ing to lower birefringence. The bistability region (**II**) around the minimum threshold has expanded, while its high frequency border bends towards the threshold line. However, the most important difference with Fig. 1 is that now, $\hat{x}$ is stable on almost the whole blue side of the gain peak for high enough currents. This is due to a new border running quite parallel to the threshold line from the low-frequency border of **II** towards the blue side of the gain peak. This border, which in fact was already present in Fig. 1 though at quite high current values, becomes closer to the threshold line as either γ_p or γ_j decrease. Finally, in some cases (not shown in Fig. 2) another region may appear where neither of the linearly polarized modes is stable as described elsewhere.[11]

As before, PS occurs as the system is brought from **I** to **III** or viceversa. However, there are now *two possible, independent ways* to achieve this goal. The first one is, as before, "thermally induced" since it corresponds to scanning Δ. The second is to keep constant Δ while increasing I. We call this second mechanism "non-thermal" since it occurs at constant Δ and while staying on the blue side of the gain peak. It is associated with the polarization switching mechanisms discussed in Ref. [11]. It should be noted that in this case, the switching takes place from the LP mode with the longer wavelength to that with shorter wavelength, i. e., from the larger to the smaller unsaturated gain.

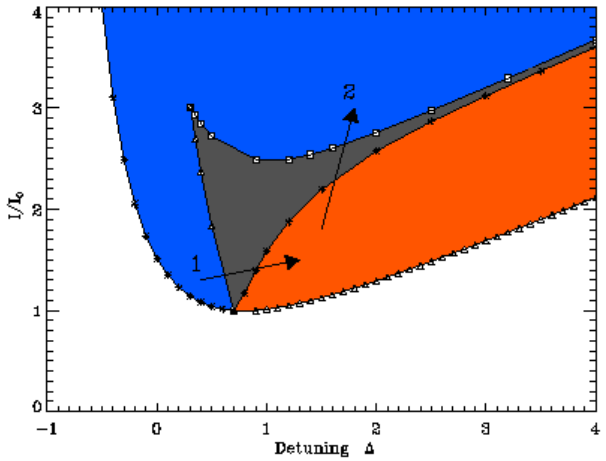

Fig. 2. Stability diagram of linearly polarized solutions. Solid arrows indicate possible switching processes (see text). Same parameter values than in Fig. 1 except for $\gamma_p = 3\ ns^{-1}$.

The most general stability diagram in Fig. 2 can be readily connected to different experimental situations. When the injection current is slowly increased, the temperature of the device also increases following the current injection due to self-heating, which is only effective on relatively long time-scales ($\sim 1\mu s$). Then, a diagonal path in the $I-\Delta$ stability diagram is followed. For VCSELs with large spectral shift of the cavity resonance relative to the gain spectrum the path is quite "horizontal" and therefore only the PS associated to arrow 1 can be observed. If the thermal shift of the cavity resonance and gain spectrum were smaller, then the path would be more "vertical" and the PS along arrow 2 could be observed under quasi CW operation. In any case, experiments where the current increases on times shorter than the thermal response time can explore these transitions occurring for constant Δ[9].

In summary, we have shown that polarization switching in single-transverse mode VCSELs can in general be induced in two independent ways. The linearly polarized states of a VCSEL are associated to a phase-locked state of the two circularly polarized components of the optical field, $E_\pm$, at either $\phi = 0$ or π. Polarization switching occurs associated to the exchange of stability of these phase-locked states through amplitude-phase coupling, which can be achieved by either increasing the injection current at constant detuning or by scanning the detuning while keeping the injection current fixed. The latter case can be termed a thermally induced polarization switching since the primary thermal effect is to redshift in different amounts the cavity resonance and the gain spectrum. On the contrary, the former one is not thermally induced, and it relies on the saturable dispersion effect associated with the carrier and frequency dependence of the refractive index of the active region.

Work partially supported by the European Commission (TMR Project FMRX-CT96-0066) and by DGICYT and CICYT (Spain) Projects PB94-1167 and TIC98-0418.

1. See the reviews by M. San Miguel, K. Ebeling and O. Blum in *Semiconductor Quantum Optoelectronics*, Ed. A. Miller, Institute of Physics (1999).
2. Z.G. Pan, S. Jiang and M. Dagenais, R.A. Morgan, K. Kojima, M.T. Asom, R.E. Leibenguth, G.D. Guth and M.W. Focht, Appl Phys. Lett. **63**, 2999 (1993)
3. H. Kawaguchi, I. S. Hidayat, Y. Takahashi and Y. Yamayoshi, Electron. Lett. **31**, 109 (1995)
4. K. D. Choquette, K. L. Lear, R. L. Leibenguth, and M. T. Ason, Appl Phys. Lett. **64**, 2767 (1994)
5. K. Panajotov, B. Ryvkin, J. Danckaert, M. Peeters, H. Thienpont and I. Veretennicoff, IEEE Photon. Technol. Lett., **10**, 6 (1998).
6. K. D. Choquette, R. P. Schneider Jr., K. L. Lear and R. E. Leibenguth, IEEE J. Select. Topics Quantum Electron., **1**,661 (1995).

7. K. D. Choquette, K. L. Lear, R. P. Schneider Jr., R. E. Leibenguth, J. J. Figiel, S. P. Kilcoyne, M. Hagerott-Crawford and J. C. Zolper, in "Laser Diodes and Aplications", SPIE Proceedings, Vol. 2382, 125-136 (1995).
8. A. Valle, K. A. Shor, and L. Pesquera, IEEE J. of Lightwave Technol., **14**, 2062 (1996).
9. J. Martín-Regalado, J. L. A. Chilla, J. J. Rocca and P. Brusenbach, Appl. Phys. Lett. **70**, 3350 (1997).
10. M. SanMiguel and Q. Feng and J. V. Moloney, Phys. Rev. A, **52**, 1728 (1995).
11. J. Martín-Regalado, M. SanMiguel, N.B. Abraham and F. Prati, IEEE J. Quantum Electron.,**33**, 765 (1997); J. Martín-Regalado, S. Balle, M. San Miguel, A. Valle and L. Pesquera, Quantum and Semiclass. Opt. **9**, 713 (1997).
12. R. S. Britton, T. Grevatt, A. Malinowski, R. T. Harley, P. Perozzo, A. R. Cameron and A. Miller, Appl. Phys. Lett. **73**, 2140 (1998).
13. H. Haug and S. Schmitt-Rink, Prog. Quantum Electron. Vol. 3 (1984); M. Lindberg and S. W. Koch, Phys. Rev. B **38**, 3342 (1988).
14. S. Balle, Phys. Rev. A, **57**, 1304 (1998).